Bypass Transition in Compressible Boundary Layers

J. J. Van der Vegt

1. Motivation and Objectives

Transition to turbulence in aerospace applications usually occurs in a strongly disturbed environment. For instance, the effects of free-stream turbulence, roughness and obstacles in the boundary layer strongly influence transition. Proper understanding of the mechanisms leading to transition is crucial in the design of aircraft wings and gas turbine blades, because lift, drag and heat transfer strongly depend on the state of the boundary layer, laminar or turbulent. Unfortunately, most of the transition research, both theoretical and experimental, has focused on natural transition. Many practical flows, however, defy any theoretical analysis and are extremely difficult to measure. Morkovin[5] introduced in his review paper the concept of bypass transition as those forms of transition which bypass the known mechanisms of linear and non-linear transition theories and are currently not understood by experiments.

In an effort to better understand the mechanisms leading to transition in an disturbed environment, experiments are conducted studying simpler cases, viz. the effects of free-stream turbulence on transition on a flat plate, Sohn and Reshotko[14] and Wang et al.[19]. It turns out that these experiments are very difficult to conduct, because the generation of free-stream turbulence with sufficiently high fluctuation levels and reasonable homogeneity is non trivial. For a discussion see Morkovin[5]. Serious problems also appear due to the fact that at high Reynolds numbers the boundary layers are very thin, especially in the nose region of the plate where the transition occurs, which makes the use of very small probes necessary.

The effects of free-stream turbulence on transition are the subject of this research and are especially important in a gas turbine environment, where turbulence intensities are measured between 5 and 20%, Wang et al.[19]. Due to the fact that the Reynolds number for turbine blades is considerably lower than for aircraft wings, generally a larger portion of the blade will be in a laminar-transitional state. Turner[15] shows that the effect of free-stream turbulence on transition significantly increases when the free-stream turbulence levels become larger than 5% and is accompanied with a significant increase in heat transfer. Recently Rai and Moin[11] presented a direct numerical simulation of transition to turbulence on a flat plate in a free-stream with Mach number .1 and turbulence levels at the leading edge of about 2.75%. Direct numerical simulations offer a unique opportunity to study specific phenomena, while excluding disturbances from other sources. The computations from Rai and Moin show some impressive results, especially regarding intermittency and turbulent spots. Their numerical simulation, however, has the same problem as with most of the experiments, namely a very low Mach number,

while many applications operate in the transonic regime. Due the nature of their numerical scheme, a non-conservation formulation of the Navier-Stokes equations, it is a non-trivial extension to compute flow fields in the transonic regime.

This project aims at better understanding the effects of large free-stream turbulence in compressible boundary layers at Mach numbers both in the subsonic and transonic regime using direct numerical simulations. The present project aims at computing the flow over a flat plate and curved surface. This research will provide data which can be used to clarify mechanisms leading to transition in an environment with high free stream turbulence. This information is useful for the development of turbulence models, which are of great importance for CFD applications, and are currently unreliable for more complex flows, such as transitional flows.

2. Accomplishments

Direct simulations of transition in compressible flows with both shocks and boundary layers requires an extremely accurate and efficient scheme. Several conflicting requirements present a serious challenge which cannot be met by existing numerical schemes:

- The small grid spacing in the boundary layer makes an implicit scheme necessary, because an explicit scheme would have a severe time step limitation. Implicit schemes usually are not time accurate and rather dissipative.
- Higher order accurate schemes are necessary but higher order accurate schemes generally do not give non-oscillatory solutions around discontinuities, such as shocks. Many of the popular non-oscillatory shock capturing schemes, such as TVD (Total Variation Diminishing) methods, are only first order accurate in multi-dimensional flows and even in one-dimension they reduce to first order at non-sonic local extrema.

In order to satisfy these conflicting requirements a significant effort has been made to improve and combine several successful numerical schemes. A fully implicit and time accurate code for the solution of the three-dimensional compressible Navier-Stokes equations in general geometries has been written and tested. Higher order accuracy and shock capturing are implemented using an Essentially Non-Oscillatory (ENO) scheme. Time accuracy is obtained using a Newton method.

In the next section a brief description of the numerical scheme will be given followed by the discussion of a series of tests aimed at validating the code.

2.1 Numerical Scheme

The compressible Navier-Stokes equations are solved using a finite volume method. A detailed discussion of finite volume and difference methods can be found in Vinokur[18]. The integral formulation of the Navier-Stokes equations, assuming all variables are continuous in time, is given by:

$$\frac{\partial}{\partial t}\int_{V(t)} \mathbf{U} dV + \oint_{S(t)} \mathbf{n}\cdot\mathcal{F} dS = 0 \qquad (2.1.1)$$

Here $V(t)$ and surface $S(t)$ are the volume and outer surface of the domain Ω and $\mathbf{n}$ an outward unit normal vector at S. The vector $\mathbf{U}$ represents the conserved variables: $(\rho, \rho u, \rho v, \rho w, e)^T$, with ρ the density, u, v and w the velocity components, and e the total energy. The tensor $\mathcal{F}$ is defined as $\mathcal{F} = \mathcal{E} + \mathcal{V}$, with $\mathcal{E}$ the inviscid contribution defined as:

$$\mathbf{E}_1 = \begin{pmatrix} \rho u \\ \rho u^2 + p \\ \rho uv \\ \rho uw \\ (e+p)u \end{pmatrix}; \quad \mathbf{E}_2 = \begin{pmatrix} \rho v \\ \rho uv \\ \rho v^2 + p \\ \rho vw \\ (e+p)v \end{pmatrix}; \quad \mathbf{E}_3 = \begin{pmatrix} \rho w \\ \rho uw \\ \rho vw \\ \rho w^2 + p \\ (e+p)w \end{pmatrix} \tag{2.1.2}$$

and $\mathcal{V}$ the viscous contribution:

$$\mathbf{V}_1 = \begin{pmatrix} 0 \\ \tau_1 \\ \mathbf{u} \cdot \tau_1 + q_1 \end{pmatrix}; \quad \mathbf{V}_2 = \begin{pmatrix} 0 \\ \tau_2 \\ \mathbf{u} \cdot \tau_2 + q_2 \end{pmatrix}; \quad \mathbf{V}_3 = \begin{pmatrix} 0 \\ \tau_3 \\ \mathbf{u} \cdot \tau_3 + q_3 \end{pmatrix} \tag{2.1.3}$$

The shear stress tensor $\mathcal{T}$, with components (τ_1, τ_2, τ_3) is defined as:

$$\mathcal{T} = \frac{1}{Re}(\mu(\nabla \mathbf{u} + \nabla \mathbf{u}^T) + \lambda(\nabla \cdot \mathbf{u})\mathcal{I}) \tag{2.1.4}$$

and the heat flux $\mathbf{q}$ as:

$$\mathbf{q} = \frac{\kappa \nabla T}{(\gamma - 1) Re M_\infty^2 Pr} \tag{2.1.5}$$

The variables p, T, μ, λ and κ represent the pressure, temperature, first and second viscosity coefficient and thermal conductivity, respectively. The coefficients Re, M_∞, and Pr are the Reynolds, Mach, and Prandtl numbers. All variables are non-dimensionalized using free-stream variables and a characteristic length L.

The Navier-Stokes equations are solved using a finite volume method because we seek a weak solution in order to capture shocks in high Reynolds number flows. The finite volume method is also the most natural way to satisfy the conservation properties of the differential equations. After subdividing the volume V into a set of disjunct cells we obtain the finite volume discretization for a cell with index i, j, k:

$$\frac{\partial}{\partial t}\left(V \overline{\mathbf{U}}_{i,j,k}\right) + \hat{\mathbf{F}}^1_{i+\frac{1}{2},j,k} - \hat{\mathbf{F}}^1_{i-\frac{1}{2},j,k} + \hat{\mathbf{F}}^2_{i,j+\frac{1}{2},k} - \hat{\mathbf{F}}^2_{i,j-\frac{1}{2},k} + \hat{\mathbf{F}}^3_{i,j,k+\frac{1}{2}} - \hat{\mathbf{F}}^3_{i,j,k-\frac{1}{2}} = \mathbf{0} \tag{2.1.6}$$

where a barred quantity with index i, j, k is an average of the unbarred quantity over the cell with index i, j, k and indices $i \pm \frac{1}{2}$, $j \pm \frac{1}{2}$ and $k \pm \frac{1}{2}$ refer to values at the cell faces. The fluxes $\hat{\mathbf{F}}^i$ at the cell faces are defined as:

$$\hat{\mathbf{F}}^l = \mathbf{S}^l \cdot \mathcal{F} \tag{2.1.7}$$

with $\mathbf{S}^l$ the cell face in the direction i. The computation of the cell face $\mathbf{S}^l$ and volume V has to be done with great care in order satisfy the geometric conservation law, for details see Vinokur[19]:

Flux Approximation

The crucial part in the development of a finite volume method is the approximation of the fluxes at the cell faces. The flux $\hat{\mathbf{F}}^1_{i+\frac{1}{2}}$ is computed using the Osher approximate Riemann solver. The first order accurate conservative flux is given by:

$$\hat{\mathbf{F}}^1_{i+\frac{1}{2},j,k} = \frac{1}{2}(\hat{\mathbf{F}}^1_{i,j,k} + \hat{\mathbf{F}}^1_{i+1,j,k} - \int_{\Gamma^i} |\partial\hat{\mathbf{F}}^1| du) \tag{2.1.8}$$

with equivalent expressions for the other two directions. The integral is computed along a path in phase space, connecting the points with index (i,j,k) and $(i+1,j,k)$. Along each subpath a Riemann problem is solved, which is used to determine the intermediate states. In this way exact expressions can be derived for the path integrals. More details about the implementation of the Osher scheme can be found in Osher and Solomon[6], Osher and Chakravarthy[7], Chakravarthy and Osher[1] and Rai and Chakravarthy[10]. The Osher approximate Riemann solver is the most accurate approximate Riemann solver and satisfies the entropy condition, contrary to the Roe approximate Riemann solver which needs an entropy fix to eliminate steady expansion shocks. The Osher scheme captures steady shocks in at most two points.

The most important reason for the choice of the Osher scheme, however, has been its low numerical dissipation in boundary layers, Koren[4]. Most schemes for the Euler equations are very dissipative in the boundary layer and not well suited for direct numerical simulations. In earlier work, Van der Vegt[17], modifications to flux vector splitting schemes were discussed to alleviate this problem, but although significant improvement was achieved on steady laminar boundary layers, it was not possible to reach accuracy levels necessary for direct simulations.

Higher order spatial accuracy

Direct simulations require a high accuracy which cannot be achieved with standard second order schemes. It is fairly straightforward to derive higher order accurate finite difference schemes, but shock capturing then will not be possible. The development of higher order accurate, multi-dimensional finite volume schemes, capable of shock capturing still is an area of active research, and has been an important subject in this project. A significant effort has been made to combine the Osher approximate Riemann solver, discussed in the previous section, with an ENO scheme. Results of this work are described in Van der Vegt[17], where the different ENO methods are discussed and results of various tests are discussed.

Higher order accuracy of a finite volume method can be defined is various ways. One approach is to define higher order accuracy with respect to the cell averaged values. This resembles most closely the finite volume description, which gives equations for the cell averaged values. Another definition of higher order accuracy uses the point values at the cell center, which is used in conservative higher order finite difference methods. Both approaches are being used. For subsonic flows currently the fifth order scheme, developed by Rai[9], is used, which is based on a Taylor series expansion of the flux vector along the lines presented by Osher and Chakravarthy[8]. This method is a conservative finite difference scheme. It has the benefit that it is

simple to implement in more dimensions, but does not allow shock capturing. Osher and Chakravarthy[8] demonstrated how to make these schemes TVD and allow shock capturing, but they are not very useful and only first order accurate globally. The scheme therefore is used in its unlimited form, limiting its application to flows without discontinuities such as shocks. The scheme also is rather expensive and work is in progress to improve its efficiency.

For flows with shocks research has been carried out to develop higher order accurate ENO schemes. ENO schemes use an adaptive stencil where a searching algorithm tries to find that part of the flow field surrounding a cell which is the smoothest. Then a conservative, higher order accurate interpolation method is used to "reconstruct" the point values from the cell averaged values. Due to the fact that the interpolation process only uses data from the smooth part of the flow field numerical oscillations will be minimized. In this way uniform higher order accuracy can be obtained. The first ENO methods were developed by Harten et al.[3], and later modifications were proposed by Shu and Osher[12,13]. In Van der Vegt[17] the different methods were compared and it was found that the ENO scheme, using primitive function reconstruction from cell averaged variables with the Cauchy-Kowalewski procedure for time integration combined with the Osher approximate Riemann solver, was the most accurate and robust. In one dimension it has been successfully used up to fifth order accuracy, but due to the fact that in multi-dimensional flows currently dimension splitting is used, its accuracy is limited to second order in more than one dimension. Work to extend this scheme to higher order accuracy in multi-dimensional flows is in progress.

Time integration

Due to the very small gridspacing necessary at the wall and in critical layers explicit time integration would result in a serious time step limitation. To alleviate this problem implicit time integration has to be used, but most implicit time integration schemes make assumptions in the implicit part which reduce or eliminate time accuracy. The development of implicit and time accurate numerical schemes therefore has been a significant part of this research. Time accuracy is obtained using the Newton method discussed in Rai[9], which solves the non-linear system of equations in the implicit time integration scheme using a Newton method. Rai uses this method also to reduce the error caused by approximate factorization. We do not use approximate factorization but solve the whole matrix system iteratively, see Van der Vegt[16], and need the Newton scheme only to reduce the error due to the time linearization. This iterative scheme also has the benefit that it is not necessary to use an exact linearization of the flux vectors, which can be very difficult and time consuming to obtain. First order Steger-Warming flux vector splitting is used in the implicit scheme, while a higher order accurate spatial discretization is used for the explicit part. At each time step the Newton iteration is performed such that the accuracy of the higher order explicit part is maintained. The use of an approximate linearization, however, limits the maximum time step and work is in progress to evaluate if a more accurate linearization would improve the performance and robustness of the scheme. Especially at high Mach numbers there still

are convergence problems for large Courant numbers when the scheme is used to obtain steady state solutions.

2.2 Results and Discussion

Several computations have been carried out to test the code and the various numerical schemes. In order to test the Osher approximate Riemann solver and the ENO schemes a large number of shock tube calculations have been carried out, a detailed description of this work can be found in Van der Vegt[17]. The different ENO schemes tested were the ENO method from Harten et al.[3], using primitive function reconstruction and either Runge-Kutta time integration or the Cauchy-Kowalewski procedure, and the Shu and Osher flux-ENO scheme. In all cases the Osher approximate Riemann solver was used and the effect of the ordering of the eigenvalues, viz. natural and reversed ordering, has been investigated. Four cases with different difficulties were tested, see Table 1. The performance of the different schemes was reasonable in most cases, but it turned out that the ENO scheme with primitive function reconstruction and the Cauchy-Kowalewski procedure for time integration (ENO-CK) was the most accurate and robust. Some of the results obtained with this method, are shown in Figures 1 and 2. Figure 1 shows a left moving shock followed by a contact discontinuity and a right moving expansion wave. A difficult problem for the ENO schemes in case A is the fact that in the initial stages there are not enough grid points available in the region between the shock and contact or shock-shock. The ENO scheme searches for the stencil which gives the smoothest part of the flow field around a grid point or cell. In these cases there exist in both directions a discontinuity and there are not enough points available to build a non-oscillatory higher order reconstruction. This problem exist for all ENO schemes but the ENO Cauchy Kowalewski scheme is the least sensitive for it. The other methods have mild to strong oscillations in these areas. One way to solve this problem is to reduce the accuracy locally till enough grid points are available to create a higher order reconstruction, but this is a problem which still needs further attention. Case B, Figure 3, shows a left moving expansion wave and a right moving contact discontinuity and shock. One of the problems in this case is the appearance of a sonic point, which gives a small jump of $O(\Delta x)$ at first order. The shock tube tests showed that it is possible to use a higher order scheme for flows with discontinuities, but the convergence of these higher order schemes can

Case	P_L	P_R	U_L	U_R	T_L	T_R
A	15000	98400	0	0	1378	4390
B	988000	9930	0	0	2438	2452
C	10000	100000	0	0	2627	272
E	573	22300	2200	0	199	546

Table 1. Initial Conditions Shock Tube Tests.

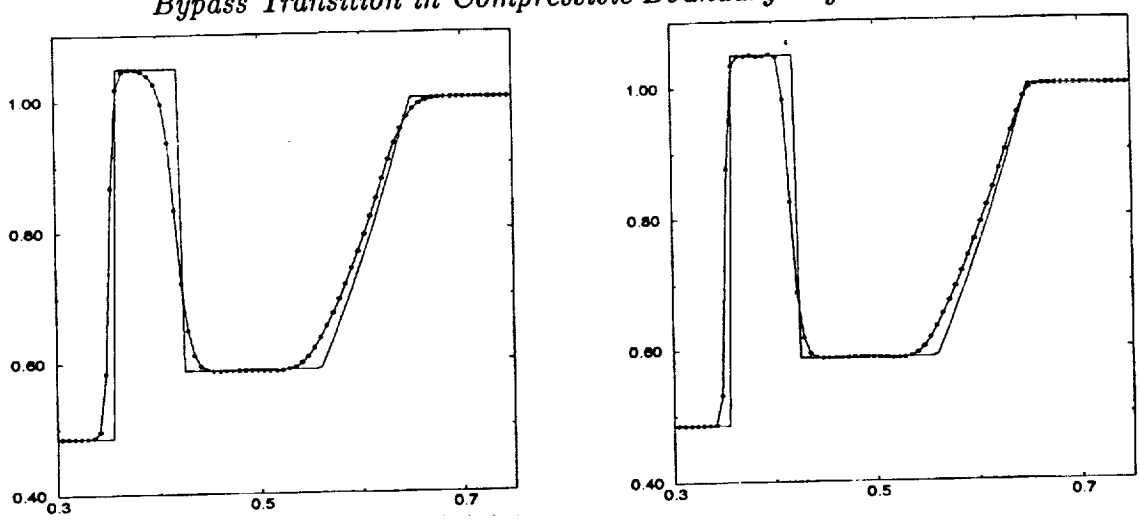

Fig. 1. Case A, density at $t = .2$, 2nd and 5th order ENO-CK.

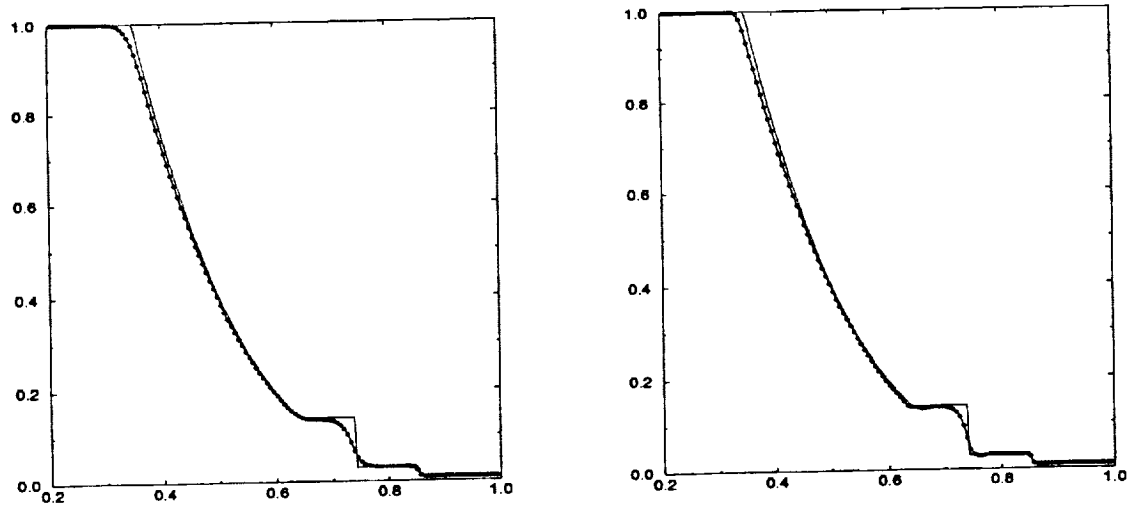

Fig. 2. Case B, density at $t = .2$, 2nd and 5th order ENO-CK.

be at most first order around these discontinuities. Tests of all the ENO schemes on smooth solutions showed that they all reached the proper level of accuracy. Test are currently underway to check if the ENO schemes give higher order accuracy in regions outside discontinuities as they are supposed to. This is an important test to see if these methods are capable of shock-turbulence interaction simulations.

In order to test the shock capturing properties of the code the flow field around a circular cylinder at Mach 8 has been computed. Although the flow field was two-dimensional the three-dimensional code was used to check if the flow field remained exactly two-dimensional and the geometric conservation law was satisfied. Figure 3. presents contours of the pressure at a spanwise station along the cylinder. The solution is the same at all stations. The flow field consists of a strong bow shock where the Mach number changes from 8 to about 2.8 behind the shock at the symmetry line. Apart from the strong shock another aspect of this case is the

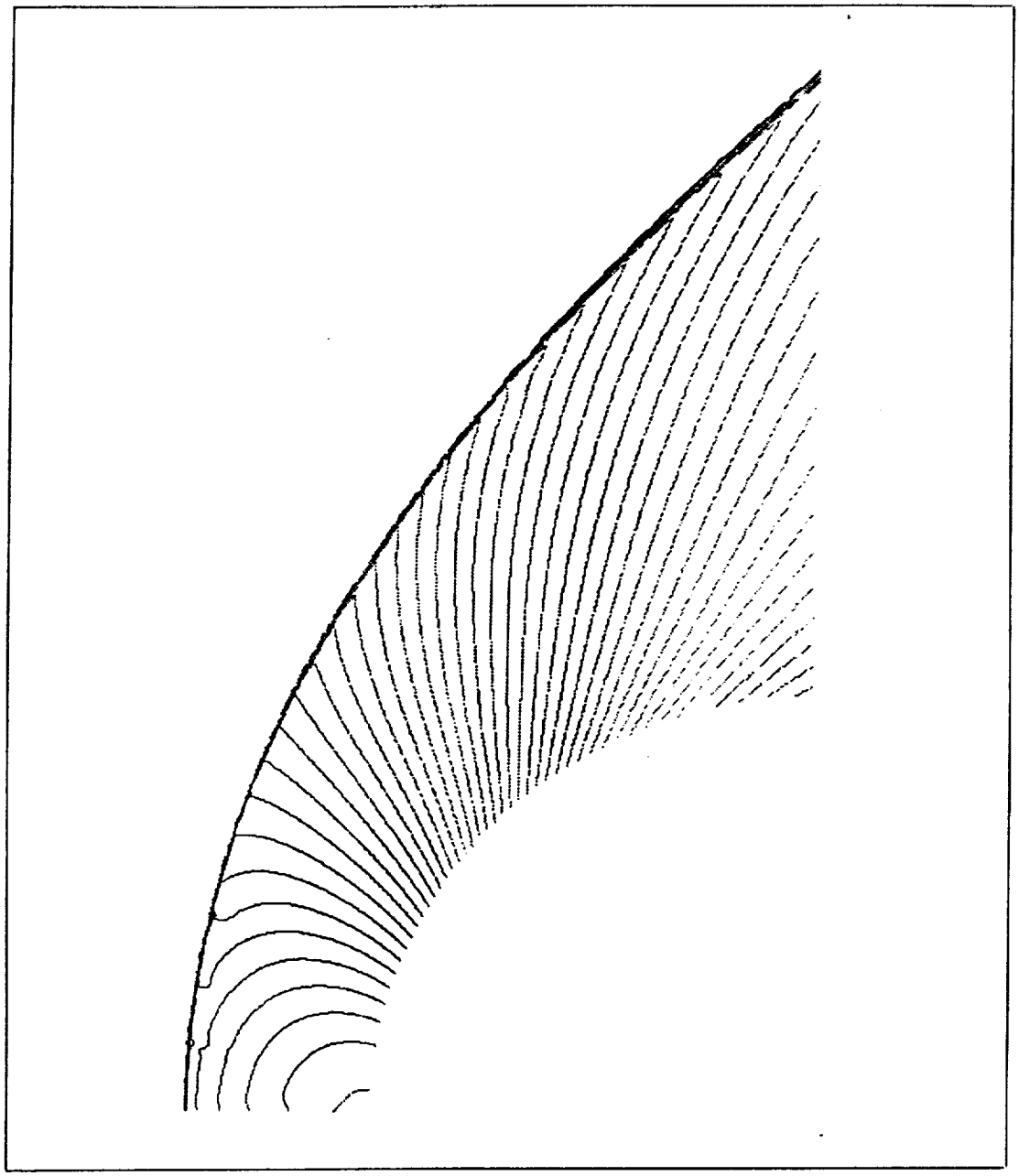

Figure 3. Pressure field of flow around a cylinder at Mach 8

fact that the flow field in the stagnation region ahead of the cylinder is subsonic. The sonic line is at about 45 degrees with the flow angle and a smooth transition is observed from the subsonic to the supersonic region. This case has also been computed by Osher and Chakravarthy[7] and the results compare well. To test the ability of the code to simulate transitional flows which is a crucial test before bypass transition can be simulated currently computations are done on natural transition in a flat plate boundary layer. A comparion is made with the results of Fasel et

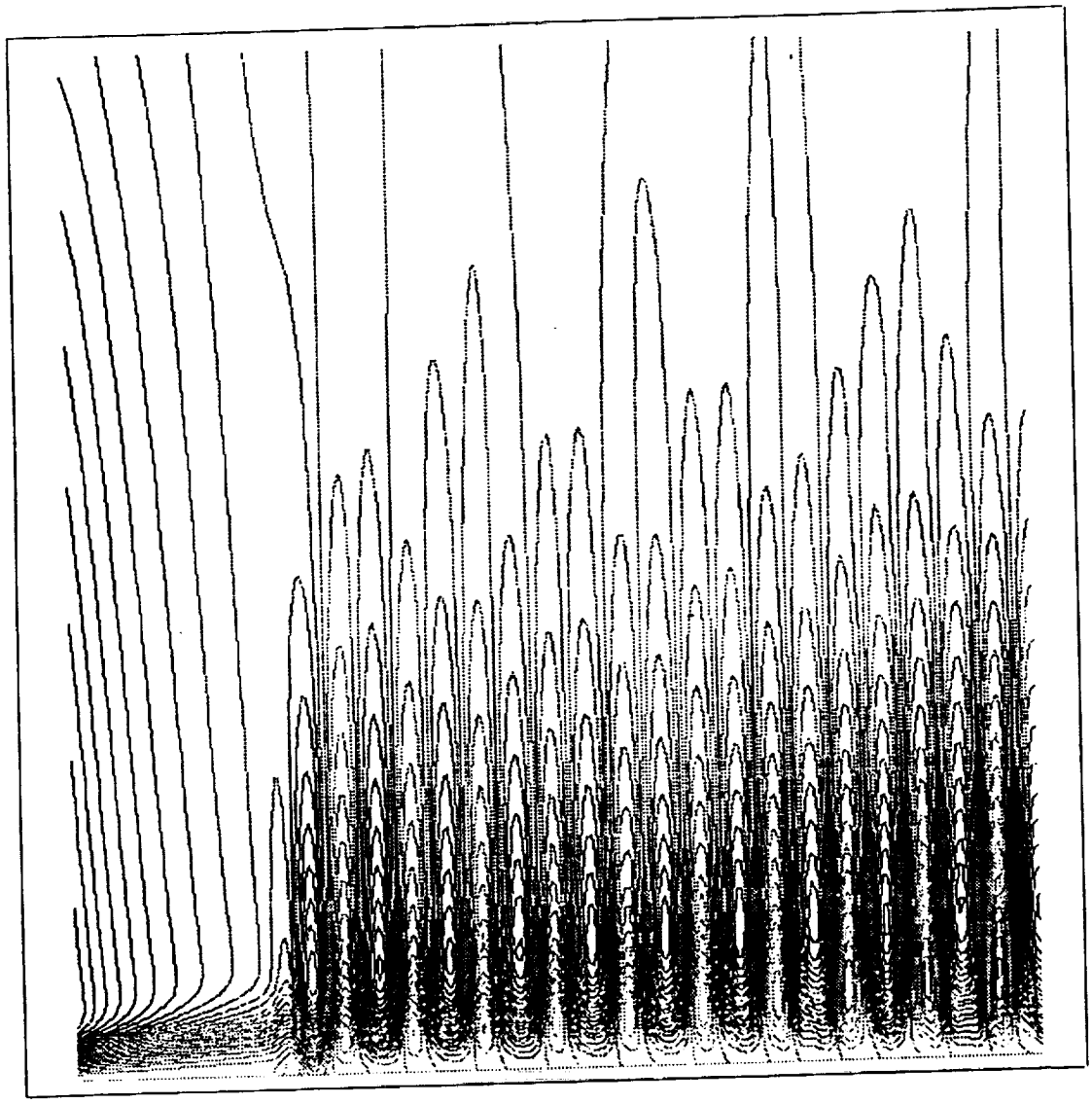

Figure 4. Vertical velocity field in a flat plate boundary layer at Mach 0.08 with periodic suction and blowing (vertical direction enlarged 20 times).

al.[2], which computed transition in an incompressible boundary layer. In order to make the comparison as accurate as possible a very low Mach number, $M_\infty = .08$ was chosen. This Mach number is approximately the lower limit for the numerical scheme and despite the fact that the computations are fully implicit a severe time step limitation is imposed by the sound waves. To start the simulation first a steady laminar boundary layer is computed, which is a non-trivial task because a very high accuracy is needed in this computation. The disturbances at the beginning of the plate have an amplitude of 10^{-4} and transition simulations require a very low numerical dissipation. The disturbances are generated by periodic suction and blowing in a strip somewhat downstream of the inflow boundary. This is done because there

are always numerical disturbances due to the fact that the inflow boundary conditions are not perfect. The disturbances are generated in a region of the boundary layer which is linearly stable. When they move downstream first the transients are damped and after they move in the unstable region the Tolmien Schlichting waves, which are the most unstable two-dimensional waves, are amplified. In order to accommodate for the fact that the subsonic outflow boundary conditions, which are essentially inviscid, are not perfect in a boundary layer a buffer layer is added to the plate to damp as much as possible the reflections coming from this boundary layer. This is the same procedure as used by Rai and Moin[11]. The number of grid points in this computation is 340×82. It turned out that the most efficient way to obtain the steady boundary layer was to first start with the second order scheme running at a Courant number of 120 using the implicit Euler time integration and to switch to the fifth order scheme after most of the transients are damped out. The fifth order scheme has a very low dissipation and would otherwise take a long time to converge. The maximum CFL number for which the fifth order scheme is stable is approximately 160. Ater the steady state was obtained periodic suction and blowing were added and the fifth order scheme was used with the Newton time integration scheme at a CFL of 60. Figure 4. shows a preliminary result of this computation and it clearly shows the gradual build up of the boundary layer instability. The results are currently analysed to make a comparison with the incompressible results of Fasel et al.[2].

3. Future Plans

Further testing of the code will have to be done for more complicated cases. Currently a comparison with the results of stability of a flat plate boundary layer at low Mach number with the results from Fasel et al.[2] is being completed. If this comparison and equivalent tests for high Mach number boundary layers are satisfactory a simulation of bypass transition on a subsonic flat plate boundary layer will be made, followed by simulations of a boundary layer on a curved plate. Also work has to be continued to develop higher order accurate ENO schemes for multi-dimensional flows. This is crucial for direct simulations of transonic flows with both shocks and turbulence.

4. References

[1] Chakravarthy, S.R. & Osher, S., "Numerical Experiments with Osher Upwind Scheme for the Euler Equations", AIAA Journal, **21**, 1241-1248, (1983).

[2] Fasel, H. F., Rist, U. and Konzelmann, U., "Numerical Investigation of the Three-Dimensional Development in Boundary-Layer Transition", AIAA Journal, **28**, 29-37, (1990).

[3] Harten, A., Engquist, B., Osher, S. & Chakravarthy, S.R., "Uniformly High Order Accurate Essentially Non-Oscillatory Schemes III", Journal of Computational Physics, **71**, 231-303, (1987).

[4] Koren, H., "Upwind Discretization of the Steady Navier-Stokes Equations", International Journal for Numerical Methods in Fluids, **11**, 99-117, (1990).

[5] Morkovin, M. V., "Bypass Transition to Turbulence and Research Desiderata in *"Transition in Turbines"*, NASA Conf. Publ. 2386, 161-204, (1984).

[6] Osher, S. & Solomon, F., "Upwind Difference Schemes for Hyperbolic Systems of Conservation Laws", Mathematics of Computation, **38**, 339-374, (1982).

[7] Osher, S. & Chakravarthy, S.R., "Upwind Schemes and Boundary Conditions with Applications to Euler Equations in General Geometries", Journal of Computational Physics, **50**, 447-481, (1983).

[8] Osher, S. & Chakravarthy, S.R., "Very High Order TVD Schemes", Mathematics and its Applications, **2**, 229-274, (1986).

[9] Rai, M. M., "Navier-Stokes Simulations of Blade-Vortex Interaction using High-Order Accurate Upwind Schemes", AIAA paper 87-0543, (1987).

[10] Rai, M.M. & Chakravarthy, S.R., "An Implicit Form for the Osher Upwind Scheme", AIAA Journal, **24**, 735-743, (1986).

[11] Rai, M. M. Moin, P., "Direct Numerical Simulation of Transition and Turbulence in a Spatially Evolving Boundary Layer", AIAA paper 91-1607-CP, (1991).

[12] Shu, C.-W. & Osher, S., "Efficient Implementation of Essentially Non-Oscillatory Shock-Capturing Schemes", Journal of Computational Physics, **77**, 439-471, (1988).

[13] Shu, C.-W. & Osher, S., "Efficient Implementation of Essentially Non-Oscillatory Shock Capturing Schemes, II", Journal of Computational Physics, **83**, 32-78, (1989).

[14] Sohn, K. H. and Reshotko, E., "Experimental Study of Boundary Layer Transition with Elevated Freestream Turbulence on a Heated Plate, NASA Contractor Report 187068, (1991).

[15] Turner, A. B., "Local Heat Transfer Measurements on a Gas Turbine Blade", J. of Mech. Eng. Sciences, **13**, 1-12, (1971).

[16] Van der Vegt, J. J. W., "Assessment of Flux Vector Splitting for Viscous Compressible Flows", AIAA paper 91-0243, (1991).

[17] Van der Vegt, J.J.W., "ENO-Osher Scheme for Euler Equations", submitted for publication, (1992).

[18] Vinokur, M., "An Analysis of Finite-Difference and Finite-Volume Formulations of Conservation Laws", Journal of Computational Physics, **81**, 1-52, (1989).

[19] Wang, T., Simon, T. W. and Buddhavarapu, J., "Heat Transfer and Fluid Mechanics Measurements in Transitional Boundary Layer Flows", in *"Transition in Turbines"*, NASA Conf. Publ. 2386, 69-79, (1984).